Available online at www.sciencedirect.com
ScienceDirect
Journal of Electroanalytical Chemistry 616 (2008) 14–26
Journal of Electroanalytical Chemistry
www.elsevier.com/locate/jelechem

Characterisation and application of carbon film electrodes in room temperature ionic liquid media

Rasa Pauliukaite [a], Andrew P. Doherty [b], Kevin D. Murnaghan [b], Christopher M.A. Brett [a,*]

[a] *Departamento de Química, Faculdade de Ciências e Tecnologia, Universidade de Coimbra, 3004-535 Coimbra, Portugal*
[b] *The School of Chemistry and Chemical Engineering, Queen's University of Belfast, David Keir Building, Stranmillis Road, Belfast, N.I. BT5AG, UK*

Received 15 March 2007; received in revised form 14 December 2007; accepted 24 December 2007
Available online 12 January 2008

Abstract

Carbon film electrodes have been characterised in the room temperature ionic liquids, 1-butyl-3-methylimidazolium bis(trifluoromethane)sulfonimide ($BmimNTF_2$), 1-butyl-1-methylpyrrolidinium bis(trifluoromethane)sulfonimide, ($BpyrNTF_2$) and 1-butyl-3-methylimidazolium nitrate ($BmimNO_3$), by cyclic voltammetry and electrochemical impedance spectroscopy. The electrochemical behaviour of the ionic liquids depended on both cation and anion of these electrolytes. Oxygen reduction is clearly visible at carbon film electrodes – after oxygen removal the potential window was wider, that of $BpyrNTF_2$ being the widest. These room temperature ionic liquids were used in the electrochemical investigation of two ferrocene derivatives, benzoyl- and acetyl-ferrocene, that are both insoluble in water and cannot be investigated in aqueous solutions. They were also applied in the investigation of two sensor and biosensor mediators, copper hexacyanoferrate and poly(neutral red), with a view to using ionic liquids as electrolytes in electrochemical sensing and biosensing systems.

Keywords: Room temperature ionic liquids; 1-Butyl-3-methylimidazolium bistriflimide; 1-Butyl-1-methylpyrrolidinium bistriflimide; 1-Butyl-3-methylimidazolium nitrate; Ferrocenes; Copper hexacyanoferrate; Poly(neutral red)

1. Introduction

Room temperature ionic liquids (RTIL) are usually organic or mixed organic–inorganic salts with a melting point lower than 100 °C. RTILs are frequently used as clean reaction media for organic synthesis [1,2]. Nevertheless, in the last few years they have become more attractive in other fields such as catalysis [1], in basic electrochemical studies of organic compounds and inorganic compounds [3–12], formation of metal nanostructures [13], analytical chemistry [14] including sensors [15–18], bioanalytical chemistry [2,19–25], and for electrochemical biosensors [26].

Application of RTILs in electrochemistry is increasing because, being inherently conducting, such systems do not require additional supporting electrolyte salt [27]. However, RTILs exhibit much higher viscosities than molecular solvents, which is caused principally by the large cationic size/asymmetry and strong inter-ionic van der Waals interactions. As a result, mass transport (diffusion) within RTILs is suppressed relative to conventional solvents [3]. Moreover, concentration-dependent diffusion has been reported: different slopes of the current dependence on concentration for ferrocene oxidation were found for low and high concentrations in 1-butyl-3-methylimidazolium bistriflimide [5,28]. The potential window in RTILs depends not only on the electrode substrate material but also on their composition and the presence of impurities (e.g. H_2O) [3,29].

Carbon film electrodes fabricated from carbon film electrical resistors have been investigated for electrochemical applications since 2001 [30]. These electrodes have been characterised [30,31] and successfully used in electroanalytical [32–36] and bioelectroanalytical studies [37–42]. These

* Corresponding author. Tel./fax: +351 239 835 295.
E-mail address: brett@ci.uc.pt (C.M.A. Brett).

0022-0728/$ - see front matter © 2008 Elsevier B.V. All rights reserved.
doi:10.1016/j.jelechem.2007.12.019

carbon film electrodes have similar electrochemical properties to glassy carbon electrodes, especially after surface pretreatment; other advantages are their physical robustness and ease of preparation.

In this work, the electrochemical behaviour of three RTILs, 1-butyl-3-methylimidazolium bis(trifluoromethane)-sulfonimide ($BmimNTF_2$), 1-butyl-1-methylpyrrolidinium bis(trifluoromethane)sulfonimide ($BpyrNTF_2$), and 1-butyl-3-methylimidazolium nitrate ($BmimNO_3$), at carbon film electrodes is reported. Their potential window at carbon film electrodes was determined using cyclic voltammetry before and after deoxygenation of the RTIL and electrochemical impedance spectroscopy measurements were performed to study the processes occurring at the electrode surface. The influence of the RTIL cation and anion is also discussed. Two ferrocene derivatives were electrochemically characterised in the RTILs, as well as carbon film electrodes modified by copper hexacyanoferrate and by poly(neutral red) prepared by in situ electropolymerisation.

2. Experimental

2.1. Chemicals and solutions

The two room temperature ionic liquids $BmimNTF_2$ and $BpyrNTF_2$ were synthesised by ion metathasis of the corresponding chloride salts with $LiNTF_2$ in acetonitrile, $BmimNO_3$ was prepared by ion metathasis of BmimCl with KNO_3 in acetonitrile. In all cases, the LiCl (or KCl) precipitate was removed by filtration and the crude IL washed ($\times 10$) with deionised water. The ionic liquids were then dissolved in acetonitrile and impurities removed with activated carbon [43]. The structure of these compounds is shown in Fig. 1.

Benzoyl- and acetyl-ferrocene were obtained from Sigma (Germany) while the neutral red monomer was purchased from Aldrich (Germany). $CuCl_2{\cdot}2H_2O$, $K_3Fe(CN)_6$ and KNO_3 were obtained from Merck (Germany); KCl was purchased from Fluka (Switzerland). Milli-Q nanopure deionised water (resistivity $\geqslant 18\ M\Omega\ cm$) was used for the preparation of aqueous solutions.

2.2. Electrode preparation

Electrodes were made from carbon film resistors ($2.0 \pm 0.1\ \Omega$ resistance) as described previously [30,31]. The resistors were fabricated from ceramic cylinders of external diameter 1.5 mm and length 6.0 mm by pyrolytic deposition of a thin carbon film. One of the tight fitting metal caps, joined to thin conducting wire, was removed from one end of the resistor and the second one was sheathed in – plastic tubing, adhered with epoxy resin. In this way, the exposed electrode geometric area was $\sim 0.20\ cm^{-2}$.

Copper hexacyanoferrate (CuHCF) was chemically deposited by immersing the electrodes for 50 min in an aqueous solution containing 10 mM $CuCl_2$, 10 mM $K_3Fe(CN)_6$, and 100 mM KCl. After this, the electrodes were dried in a hot air stream for 3 min and left for 24 h to stabilise.

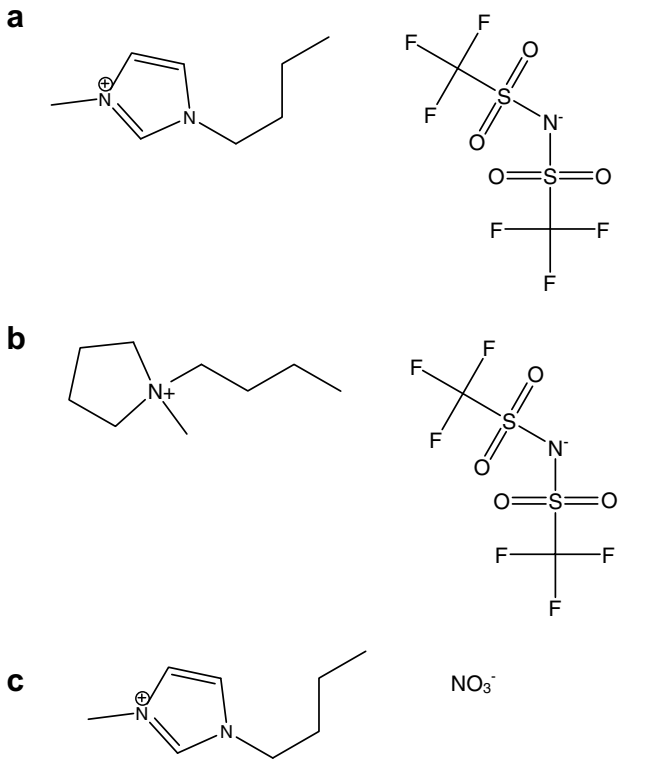

Fig. 1. Structure of ionic liquids used: (a) 1-butyl-3-methylimidazolium bistriflimide ($BmimNTF_2$); (b), 1-butyl-1-methylpyrrolidinium bistriflimide ($BpyrNTF_2$); (c) 1-butyl-3-methylimidazolium nitrate ($BmimNO_3$).

Poly(neutral red) (PNR) was deposited by electrochemical polymerisation from a 3 mM solution of its monomer (neutral red) in all three RTILs by cycling the applied potential (20 cycles at $10\ mV\ s^{-1}$) from -1.3 to $+0.8$ V (in $BmimNTF_2$), from -1.0 to $+0.75$ V (in $BpyrNTF_2$), and from -1.0 to $+1.0$ V (in $BmimNO_3$) vs. solid-state Ag/AgCl reference. In the first three cycles, the positive potential limit was extended by a further 0.3 V in order to produce radicals to initiate polymerisation. The electropolymerisation procedure in aqueous solutions is described elsewhere [44]. After preparation, PNR-coated electrodes were left in air to dry and stabilise for 24 h.

2.3. Methods and instruments

The three-electrode electrochemical cell of volume 300 μL contained a carbon film working electrode, a platinum wire as counter electrode and a silver wire covered with silver chloride as solid-state pseudo reference electrode ($Ag/AgCl_{ss}$); all measurements are given versus this electrode. Measurements were performed using a computer-controlled μ-Autolab Type II potentiostat/galvanostat with GPES 4.9 software (Eco Chemie, The

Netherlands). All solutions were deoxygenated by nitrogen bubbling for 10 min.

Electrochemical impedance measurements were carried out in the same cell with a PC-controlled Solartron 1250 frequency response analyser coupled to a Solartron 1286 electrochemical interface. A sinusoidal voltage perturbation of 10 mV amplitude was applied over the frequency range 65 kHz to 0.1 Hz with 10 measurement points per frequency decade; integration time was 60 s using short integration mode. Fitting to electrical equivalent circuits was performed with ZView 2.4 software (Solartron Analytical, UK).

3. Results and discussion

3.1. Electrochemical characterisation

3.1.1. Potential window

The cyclic voltammetric profile in all three RTILs was recorded before and after deoxygenation. Figs. 2–4 show the current–voltage response when the negative potential limit was progressively increased. Removal of oxygen had a significant effect on the profile in $BmimNTF_2$ and $BpyrNTF_2$ (Figs. 2 and 3), while in the case of $BmimNO_3$ almost no changes occurred in the cyclic voltammograms (CVs) before and after deoxygenation.

Fig. 2a shows voltammograms recorded in $BmimNTF_2$ prior to deoxygenation, where an irreversible O_2 reduction peak is observed at ~−1.0 V along with a coupled reoxidation peak at ~+0.7 V; these redox processes disappear or significantly decrease after deoxygenation, as shown in Fig. 2b. The potential window obtained, after deoxygenation, was from −2.0 to +2.0 V for $BmimNTF_2$. A similar behaviour was obtained in the case of $BpyrNTF_2$ (Fig. 3). However, the oxygen reduction peak occurs at a more negative potential (ca. −1.5 V) and is more reversible than in $BmimNTF_2$; also, the coupled oxidation peak was seen at a less positive potential of ~+0.3 V. Interestingly, reversible oxygen reduction was found at less negative potentials in $EmimNTF_2$ (1-ethyl-3-methylimidazolium bis((trifluoro-

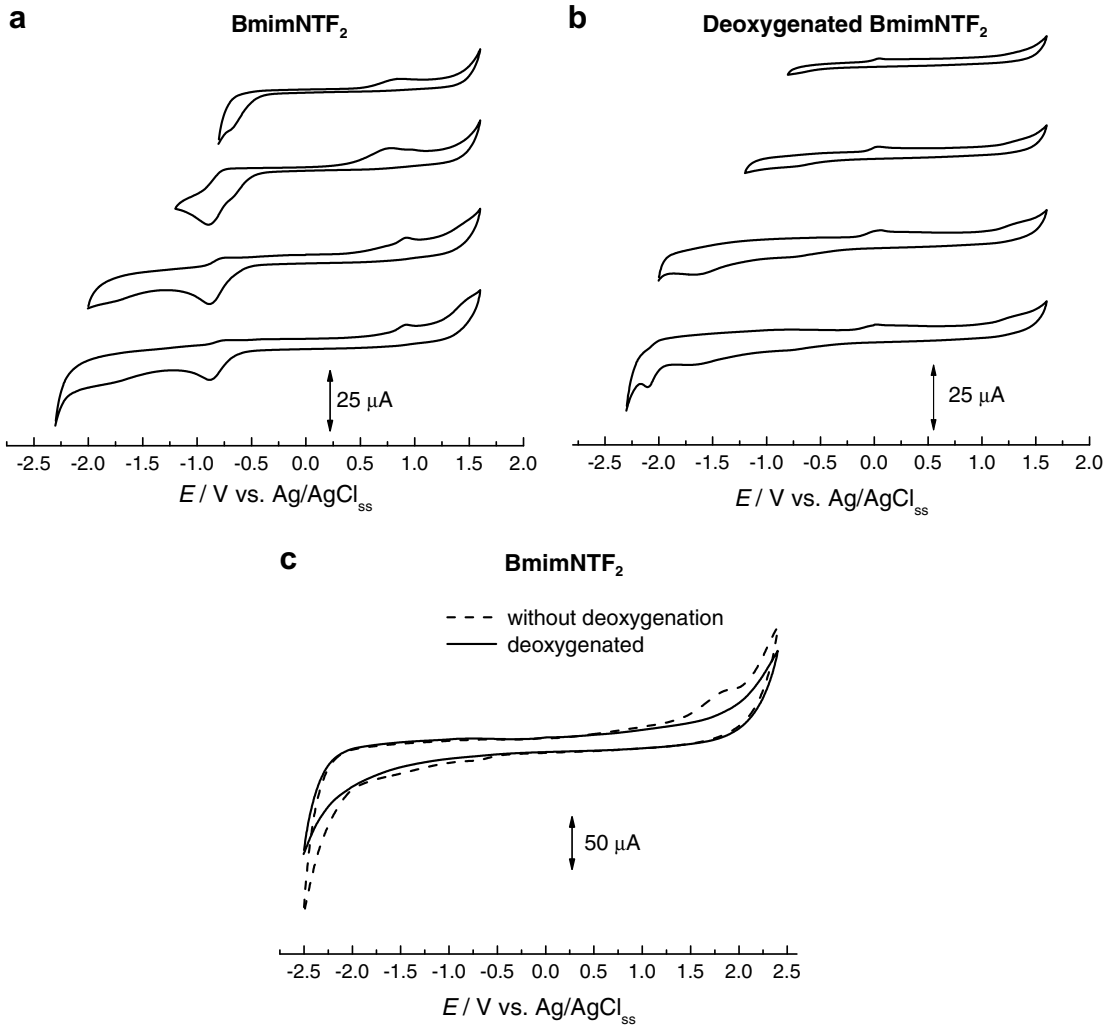

Fig. 2. Cyclic voltammograms at the carbon film electrode in $BmimNTF_2$, extending the negative potential limit step-by-step: (a) without deoxygenation, (b) after deoxygenation, (c) potential window. Scan rate 50 mV s^{-1}.

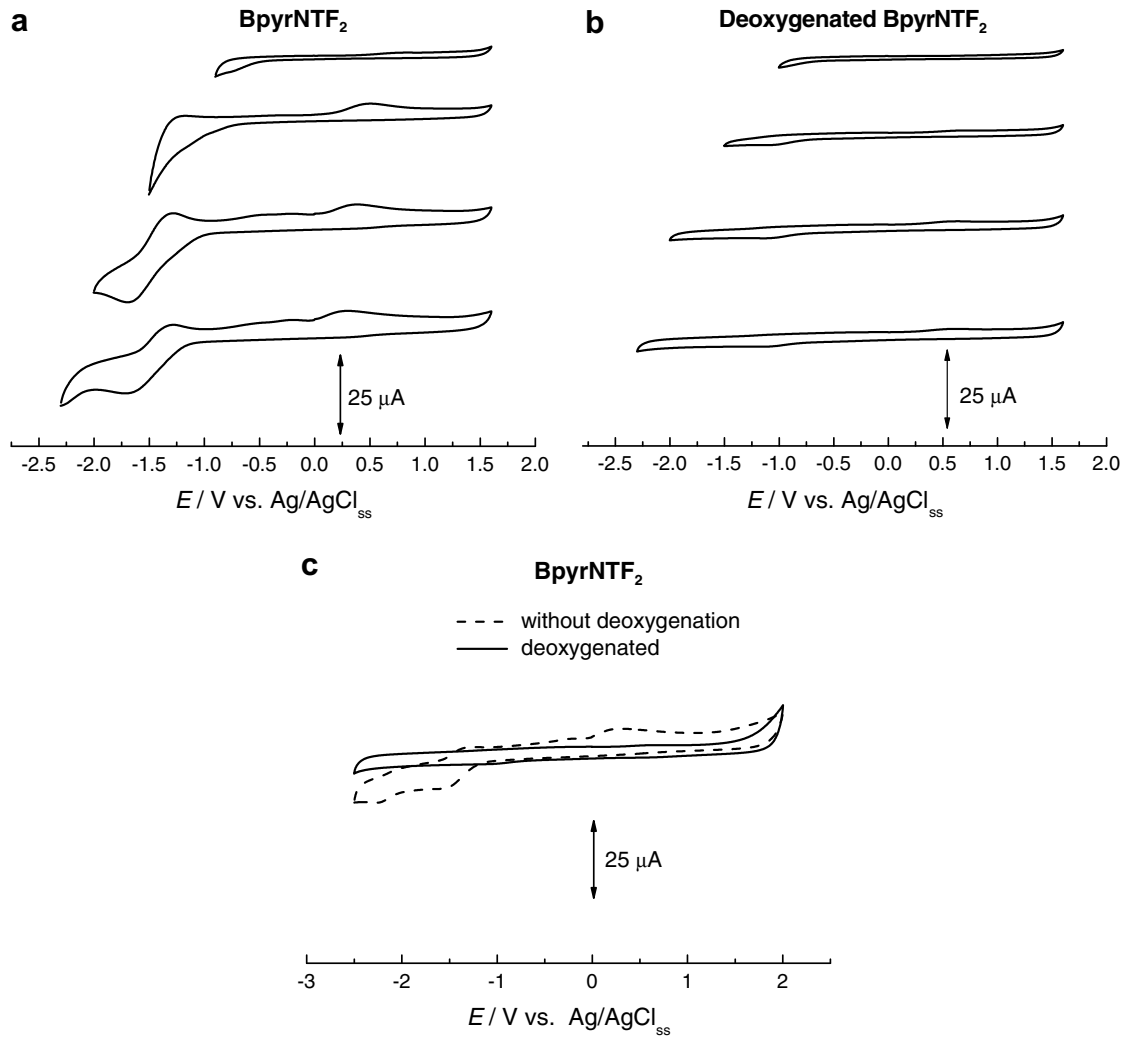

Fig. 3. Cyclic voltammograms at the carbon film electrode in $BpyrNTF_2$, extending the negative potential limit step-by step: (a) without deoxygenation, (b) after deoxygenation, (c) potential window. Scan rate 50 mV s^{-1}.

methyl)sulfonyl)imide) and $N_{6222}NTF_2$ (hexyltriethylammonium bis((trifluoromethyl)sulfonyl)imide) at a Au microdisc electrode [45]. These differences are likely to be due to the protic nature of Bmim [46] where the electrogenerated superoxide radical is protonated in Bmim. Deoxygenation of $BmpyrNTF_2$ results in the disappearance of these processes (Fig. 3b) and results in a potential window from −2.5 V to 2.0 V (Fig. 3c). However, solutions of triflimide RTILs can lead to wider potential windows, as seen at Au and Pt in 0.1 M solutions of different RTILs $EmimNTF_2$, $N_{6222}NTF_2$, and $N_{6222}PF_6$ in acetonitrile with ferrocene (Fe/Fe^+) Ref. [29].

Different electrochemical behaviour was obtained in $BmimNO_3$ (Fig. 4), where little difference due to the absence or presence of O_2 is observed. In this medium, a small reduction peak occurred at −1.5 V (Fig. 4a) which disappears upon deoxygenation (Fig. 4c) suggesting that O_2 solubility in this RTIL is low. The oxidation peaks at 0.0 V and +1.1 V in both the presence and absence of O_2 are likely to be due to the cathodic discharge products of the medium (Fig. 4a–c). For example, these peaks could be caused by reduction of NO_3^- at the electrode surface and then re-oxidation of the NO_2^- formed at positive potentials. Overall, the potential window for this liquid was found to be the narrowest, between −1.9 and +1.5 V (Fig. 4c).

Previous studies have shown that the electrochemical window reported in most ionic liquids, regardless of the reference electrode, is from 4 to 6 V [3,4,29]. Au and glassy carbon had a similar electrochemical window; however, the negative potential limit was lower in $BmimPF_6$ [4]. The potential window depended not only on the electrode substrate but also on impurities in the RTIL [3]. The potential window for $BmimNTF_2$ and $BpyrNTF_2$ dissolved in dimethyl sulphoxide was from −2.0 V to 2.6 V vs. Ag/Ag^+ at Pt, and between −3.0 V and 2.5 V vs. Ag/Ag^+ at glassy carbon, respectively [27]. $BpyrNTF_2$ led to extend a total potential window up to 6 V at graphite electrode [47]; however, it remained relatively narrow at Pt, at 3.8 V [48]. A similar potential window to that obtained at the

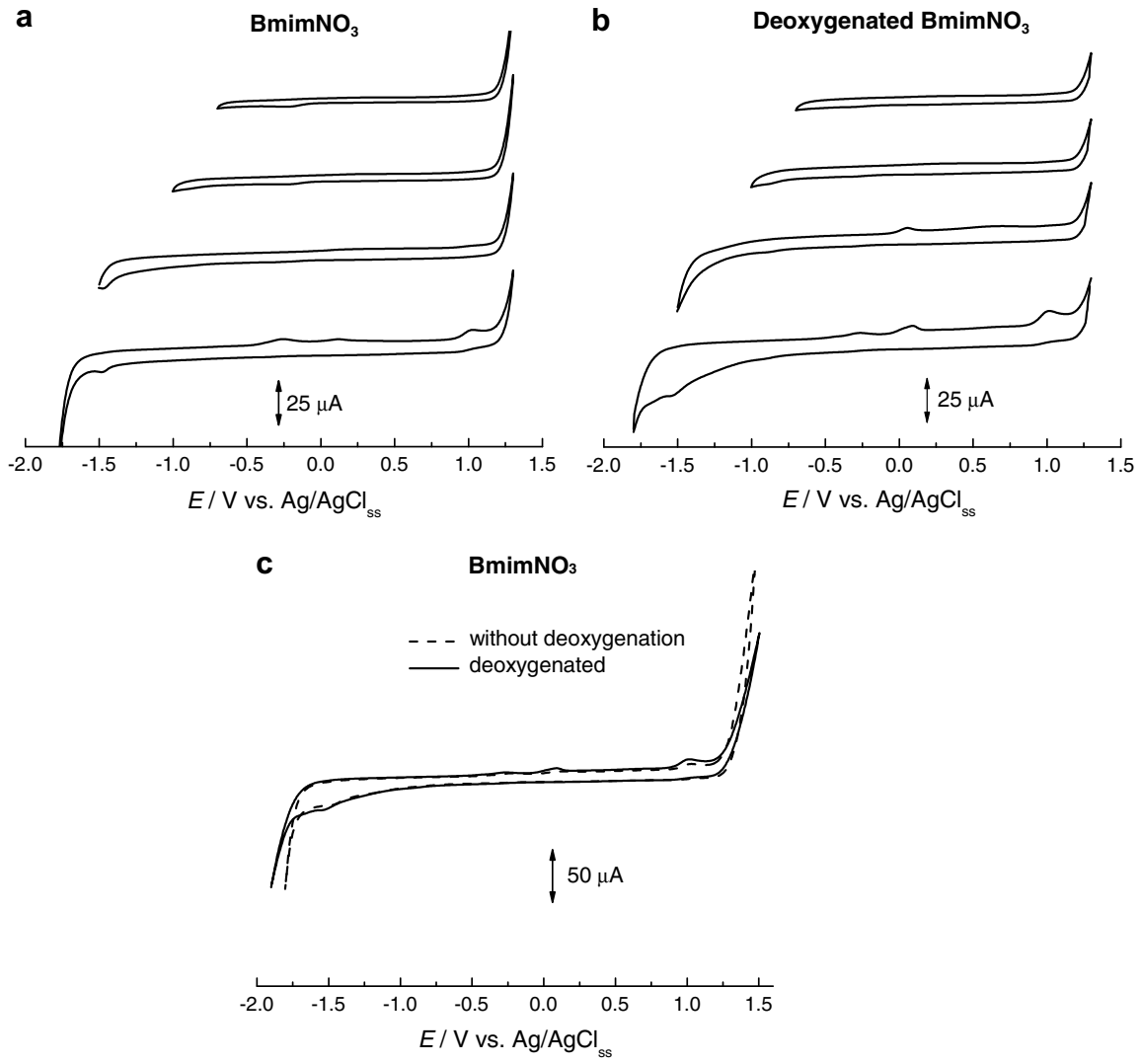

Fig. 4. Cyclic voltammograms at the carbon film electrode in $BpyrNO_3$, extending the negative potential limit step-by step: (a) without deoxygenation, (b) after deoxygenation, (c) potential window. Scan rate 50 mV s^{-1}.

carbon film electrode was found at different electrode materials, such as GC, Pt and Au in $BmimPF_6$ and $BmimBF_4$ [7,9]. Carbon nanotube electrodes in $BmimBF_4$ exhibited a narrower potential window of 3.5 V than at other carbon electrodes, including the carbon film electrode [49]. Summarising, the width of the potential window according to the electrode substrate in $BmimNTF_2$ and $BpyrNTF_2$ can be presented in the sequence: Pt < Au ⩽ CF < GC. The positive potential limit is probably determined by carbon oxidation rather than RTIL discharge at carbon film electrodes (Figs. 2 and 3). Thus, this advantage allows the application possibilities to be extended.

The conventional redox couple $Fe(CN)_6^{3-}/Fe(CN)_6^{4-}$ was studied in the RTILs (not shown) in order to determine the electroactive area of the electrode. The diffusion coefficient, obtained for this redox couple in a similar ionic liquid, $MDIM^+BF_4^-$ (1-methyl-3-[2,6-(S)-dimethylocten-2-yl]imidazolium tetrafluoroborate), was found to be 3×10^{-9} cm^2 s^{-1} [7]. Using this value, the calculated electroactive area of the carbon film electrodes in RTILs studied in this work is: ~0.12 cm^2, compared to a larger electroactive area of 0.20 cm^2 in aqueous solution [30]. This difference may be due to partial coverage of the electrode surface by the RTIL, which conditions access of the electroactive species, especially in the zones where there is nanoscale surface roughness.

3.1.2. Electrochemical impedance spectroscopy

Electrochemical impedance spectra (EIS) were recorded in deoxygenated ionic liquids over a wide potential range, from −2.0 V to +2.0 V, in steps of 0.5 V. Spectra obtained, shown in Fig. 5, show similarities with those obtained at carbon film electrodes in aqueous solutions [31].

As found in aqueous solution at carbon film electrodes, in the double layer region (0.0–0.5 V), essentially only charge separation is seen in the spectra in all three RTILs. Especially clear evidence of capacitive behaviour was found in $BpyrNTF_2$, while in the other two RTILs, lower imped-

ance values were obtained as well as a lower phase angle along with a slight curvature in the complex plane spectra. At negative potentials, the spectral shape corresponds to suppressed or regular semicircles (particularly at −1.0 and −1.5 V in $BmimNTF_2$, −1.5 V in $BmimNO_3$ and −2.0 V in $BmimNTF_2$ and $BpyrNTF_2$) due to the reduction processes (discharge of the medium) occurring at these potentials. A similar behaviour was also obtained at positive potentials due to oxidation processes (from 1.0 V to 2.0 V). Thus, at high negative and positive potentials impedance values decrease, but this decrease is not as pronounced at positive potentials as at negative potentials. Impedance spectra most similar to those in aqueous solution [31,33] were obtained in $BmimNTF_2$.

Analysis of the impedance spectra was performed by fitting equivalent electrical circuits to the experimental data. As seen from the spectra in Fig. 5, $BmimNTF_2$ had a different behaviour than the other RTILs studied and were modelled by a cell resistance (R_Ω) in series with a parallel combination of charge transfer resistance (R_1) and constant phase element ($CPE = 1/C(i\omega)^\alpha$) as a non-ideal capacitance [31] over the whole range of potentials applied.

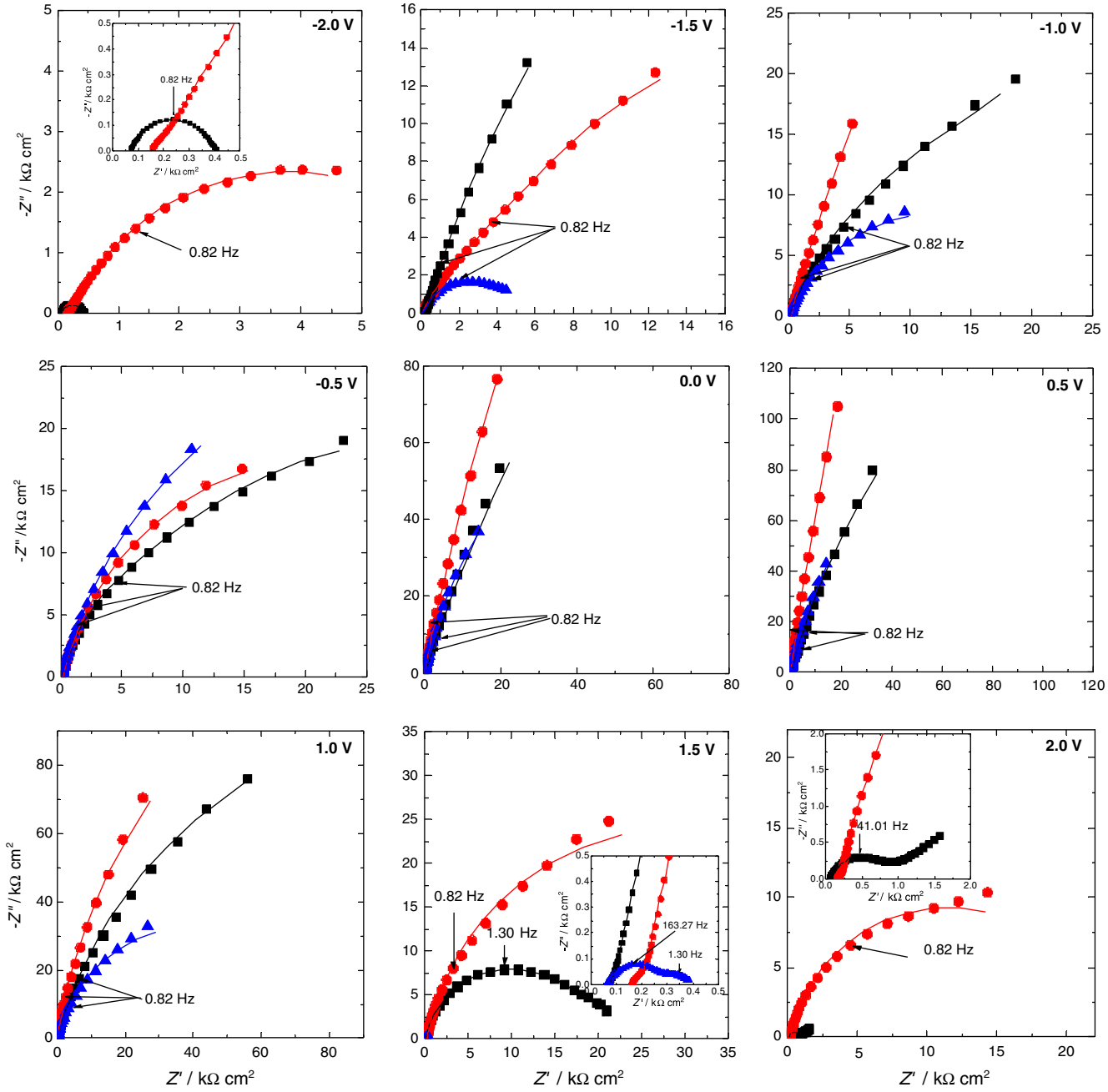

Fig. 5. Complex plane electrochemical impedance spectra at carbon film electrode at different potentials in (■) $BmimNTF_2$, (●) $BpyrNTF_2$ and (▲) $BmimNO_3$; lines show equivalent electrical circuit fitting as described in the text. All EIS conditions are described in Experimental section. Impedance values normalised by geometric area of the electrode.

The values of the parameters obtained are presented in Table 1. The values of R_Ω were ~6 Ω cm^2 for this ionic liquid. The charge transfer resistance increased from −2.0 V to 0.0 V and then decreased again up to 2.0 V. The CPE exponent, α, varied with potential from 0.7 to 0.9 similar to what is observed in aqueous solution at carbon film electrodes [31].

Impedance spectra in $BpyrNTF_2$ were more complex, except at 0.0 V and at 0.5 V, and were modelled with two *R*–CPE parallel combinations in series; one for the high frequency region and the second for the low frequency region. The spectra at 0.0 V and 0.5 V were analysed applying the same model as that for $BmimNTF_2$. The cell resistance, R_Ω, was ~7 Ω cm^2, The charge transfer resistance was low at all potentials and hardly varied in the potential region from −2.0 to −0.5 and 1.0 to 2.0 at high frequencies, while the capacitance decreased with an increase in the applied potential. The CPE exponent was similar to the case of $BmimNTF_2$, especially in the region of low frequency.

Since $BmimNO_3$ has a narrower potential window, impedance spectra were recorded only in the interval from −1.5 to 1.5 V. The same equivalent circuit model was applied as for the spectra in $BpyrNTF_2$, and the changes of the parameters were similar in both these RTILs. $BmimNO_3$ exhibited two peaks at +1.5 V, which indicates that two independent relaxation processes occur at this potential, unlike the other two ionic liquids.

Comparing the spectra from $BmimNTF_2$ and $BpyrNTF_2$, it can be seen that the cation identity has a noticeable effect on the impedance spectra. Apart from the fact that the $Bpyr^+$ cation requires fitting of a more complex equivalent circuit suggesting a more complex interfacial region with duplex character, at almost all potentials the interfacial resistance, R_1, as well as the capacitance, C_1, is lower. The spectra of $BmimNO_3$ compared with $BmimNTF_2$ show that the anion also has influence – apart from the narrower potential window which is reflected in the smaller impedance values at −1.5 V and +1.5 V, there are effects between −1.0 V and +1.0 V. Nevertheless, the spectra in $BmimNTF_2$ and in $BmimNO_3$ are almost coincident at 0.0 V and +0.5 V. In fact, this is the region of potential where there is least difference between the three RTILs tested, and the response is closest to that of a pure capacitor which implies that applications to the study of electrode processes of added electroactive species in this potential range will have least influence from the ionic liquid itself. Indeed, the double layer capacitance in $BmimNTF_2$ and $BpyrNTF_2$ at glassy carbon at these potentials has been found to be in the range of 5.2–6.9 μF cm^{-2} [27], and at carbon films it is several times higher, particularly in $BmimNO_3$, suggesting possible

Table 1
Data from the equivalent circuit fitting to the experimental impedance spectra at carbon films in different RTILs. R_1, R_2 – resistances, C_1, C_2 – capacitances, α_1, α_2 – CPE exponents

E (V) vs. SCE	R_1 (kΩ cm^2)	C_1 (μF cm^{-2} s$^{\alpha-1}$)	α_1	R_2 (kΩ cm^2)	C_2 (μF cm^{-2} s$^{\alpha-1}$)	α_2
$BmimNTF_2$						
−2.0	0.3 ± 0.0	25.3 ± 0.4	0.797 ± 0.002	–	–	–
−1.5	5.5 ± 0.1	55.2 ± 0.4	0.724 ± 0.003	–	–	–
−1.0	28.7 ± 0.5	37.2 ± 0.5	0.765 ± 0.005	–	–	–
−0.5	36.3 ± 0.1	29.0 ± 0.7	0.798 ± 0.045	–	–	–
0.0	783.9 ± 1.6	25.0 ± 0.2	0.823 ± 0.002	–	–	–
+0.5	545.9 ± 1.5	16.1 ± 0.1	0.835 ± 0.002	–	–	–
+1.0	248.9 ± 1.6	13.7 ± 0.2	0.830 ± 0.002	–	–	–
+1.5	20.6 ± 0.2	9.4 ± 0.1	0.868 ± 0.003	–	–	–
+2.0	0.7 ± 0.0	16.0 ± 0.1	0.849 ± 0.001	–	–	–
$BpyrNTF_2$						
−2.0	0.067 ± 0.008	224.0 ± 0.5	0.65 ± 0.04	7.2 ± 0.1	126.1 ± 0.1	0.736 ± 0.004
−1.5	0.065 ± 0.003	227.0 ± 0.3	0.63 ± 0.02	111.8 ± 4.3	97.6 ± 0.2	0.824 ± 0.001
−1.0	0.056 ± 0.001	203.9 ± 0.1	0.64 ± 0.01	323.3 ± 1.7	84.7 ± 0.1	0.834 ± 0.001
−0.5	0.037 ± 0.001	43.3 ± 0.1	0.82 ± 0.02	46.3 ± 0.3	40.5 ± 0.1	0.852 ± 0.001
0.0	1.369 ± 0.006	18.5 ± 0.2	0.88 ± 0.00	–	–	–
+0.5	4.418 ± 0.005	14.4 ± 0.2	0.91 ± 0.00	–	–	–
+1.0	0.045 ± 0.001	13.7 ± 0.3	0.86 ± 0.02	323.1 ± 7.0	18.6 ± 0.5	0.909 ± 0.001
+1.5	0.043 ± 0.003	13.9 ± 0.6	0.87 ± 0.04	62.6 ± 0.9	27.4 ± 0.2	0.875 ± 0.002
+2.0	0.038 ± 0.004	19.5 ± 0.1	0.85 ± 0.07	23.5 ± 0.3	26.8 ± 0.2	0.873 ± 0.003
$BmimNO_3$						
−1.5	0.049 ± 0.004	46.9 ± 0.8	0.81 ± 0.02	4.9 ± 0.0	74.8 ± 0.6	0.776 ± 0.003
−1.0	0.048 ± 0.002	50.1 ± 0.7	0.81 ± 0.02	24.3 ± 0.3	75.0 ± 0.3	0.772 ± 0.002
−0.5	0.072 ± 0.002	76.4 ± 0.7	0.73 ± 0.01	71.7 ± 0.3	58.4 ± 0.2	0.845 ± 0.001
0.0	0.081 ± 0.001	57.2 ± 0.3	0.73 ± 0.01	234.7 ± 0.4	35.6 ± 0.5	0.872 ± 0.001
+0.5	0.067 ± 0.001	42.3 ± 0.3	0.77 ± 0.01	365.6 ± 1.1	31.2 ± 0.6	0.867 ± 0.001
+1.0	0.048 ± 0.002	19.1 ± 0.4	0.85 ± 0.03	82.0 ± 0.1	25.7 ± 0.4	0.861 ± 0.002
+1.5	0.218 ± 0.003	29.6 ± 0.7	0.75 ± 0.02	1.1 ± 0.0	20.2 ± 0.7	0.679 ± 0.003

application of these ionic liquid/carbon film electrode systems as an electrochemical capacitor, an idea put forward in [27].

3.2. Applications

RTILs are known as good solvents for organic compounds, especially for those that are sparingly soluble in aqueous solutions. $BmimNTF_2$ and $BpyrNTF_2$ have already been used in the investigation of ferrocene [4,50] and benzaldehyde [5,6]. Here, the electrochemical behaviour of two ferrocene derivatives, copper hexacyanoferrate modification and the electropolymerisation of neutral red, were investigated at carbon film electrodes in the RTILs studied.

3.2.1. Electrochemical behaviour of ferrocene derivatives in RTILs

Benzoyl ferrocene (2 mM) was added to each of the RTILs and CVs were recorded at different potential scan rates. One irreversible oxidation peak of ferrocene was obtained in $BmimNTF_2$ at +0.85 V that is probably due to deprotonation of the benzoyl group and subsequent polymerisation of the deprotonated species, as found in aqueous alkaline solutions [51], and a badly-defined reduction peak at +0.2 V was visible only at scan rates lower than 3 mV s^{-1}. The oxidation peak current for this process increased linearly with increasing scan rate (not shown) with slope 29 nA mV^{-1} s, indicating that the process is controlled by adsorption of the electroactive species at the electrode surface. Also, a ferrocene redox couple was observed between −0.6 V and −0.5 V, but it was badly defined and was shifted to negative potentials compared to the same process in aqueous solutions (Fig. 6a).

A different benzoyl ferrocene behaviour was found in $BpyrNTF_2$, Fig. 6b: the redox couple was quasi-reversible and a clear increase in peak current was obtained at sweep rates from 5 to 25 mV s^{-1}, while it increased much more slowly at higher potential scan rates. However, a linear increase in current at slow scan rates was obtained as a function of the square root of the sweep rate (not shown) with slopes 385 and −311 nA $mV^{-1/2}$ $s^{1/2}$ for cathodic and anodic peaks, respectively, indicating that the process is diffusion controlled. The oxidation peak of benzoyl ferrocene in $BpyrNTF_2$ was at the same position as in $BmimNTF_2$, at +0.85 V, and the reduction peak was found to be at +0.65 V.

Although benzoyl ferrocene had a different electrochemical behaviour in $BmimNO_3$ than in the other two RTILs (see Fig. 6c), the redox peaks increased linearly with scan rate (not shown) with slopes of 32 and −32 nA mV^{-1} s. The slopes are similar to those obtained in $BmimNTF_2$.

Besides benzoyl ferrocene, acetyl ferrocene was also studied. The CVs are presented in Fig. 7. They were different in each ionic liquid, as in the case of benzoyl ferrocene, but acetyl ferrocene exhibited better reversibility. In

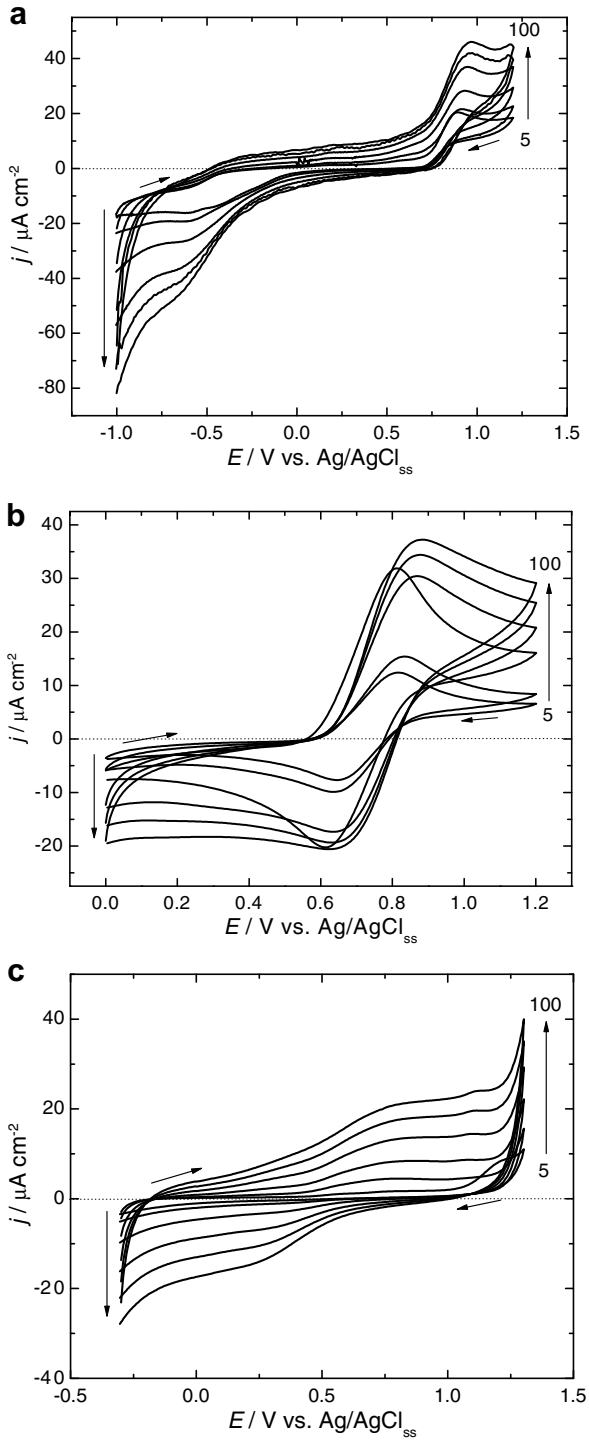

Fig. 6. Cyclic voltammograms of 2 mM benzoyl ferrocene at carbon film electrode in (a) $BmimNTF_2$, (b) $BpyrNTF_2$ and (c) $BmimNO_3$ at different scan rates: 5, 10, 25, 50, 75 and 100 mV s^{-1}.

$BmimNTF_2$, Fig. 7a, one poorly-defined ferrocene redox couple with broad peaks was obtained between +0.10 V and +0.15 V. An irreversible oxidation peak was obtained at +0.72 V with almost no dependence on scan rate and is probably due to oligomer formation between the molecules of acetyl ferrocene.

Two redox couples were obtained in $BpyrNTF_2$, Fig. 7b, in similar potential regions as those in $BmimNTF_2$, the first for ferrocene oxidation/reduction and the second, between +0.77 V and +0.85 V, was attributed to the formation of oligomers. The peak separation was around 70 mV for the second process indicating a one electron process. As in the previous case, analysis of the ferrocene redox couple is complicated due to the broad nature of the peaks, but the second one, at ~+0.8 V, the peak currents were a linear function of the square root of scan rate with slopes of 54 and −46 nA $mV^{-1/2}$ $s^{1/2}$, for oxidation and reduction peaks, respectively.

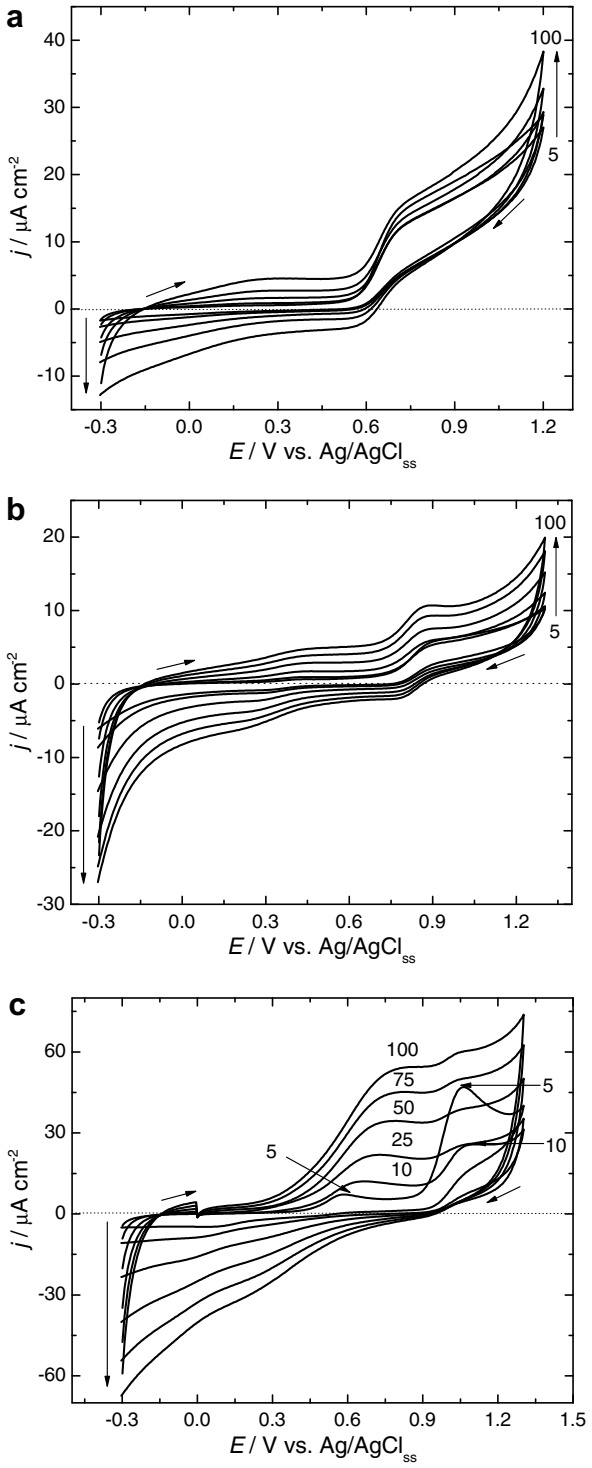

Fig. 7. Cyclic voltammograms of 2 mM acetyl ferrocene at carbon film electrode in (a) $BmimNTF_2$, (b) $BpyrNTF_2$ and (c) $BmimNO_3$ at different scan rates: 5, 10, 25, 50, 75 and 100 mV s^{-1}.

Significantly different CVs were obtained for acetyl ferrocene in $BmimNO_3$, Fig. 7c, and their shape changed with the potential scan rate. Two redox couples were also found as in the other two RTILs. The ferrocene redox couple, situated between +0.02 and +0.70 V, was irreversible as was observed for this compound in aqueous solution at low pH [50]. The other oxidation peak occurred at a more positive potential (~1.05 V), but, although well-defined, was irreversible at low potential scan rate. The acetyl ferrocene redox peaks were shifted to more positive potentials with increasing scan rate such that the oxidation peaks almost overlap with the oligomer-formation peak at scan rates higher than 100 mV $s-^{1}$. The latter decreased in height with increase in potential scan rate and a broad reduction peak appeared, making it difficult to analyse the second redox couple due to the decrease in peak current and the changes in its shape. However, the first well-defined redox couple exhibited a linear dependence on the square root of scan rate, slope 247 nA $mV^{-1/2}$ $s^{1/2}$, showing that the process was diffusion-controlled. The reduction peak was too broad and not sufficiently well-defined to be analysed.

Comparing the results obtained for ferrocene and cobaltocene redox process at different electrodes, a well-defined redox behaviour of these compounds was obtained in $BmimPF_6$ at glassy carbon conventional and Pt microdisc electrodes: transient voltammograms rather than steady-state ones were observed at the microelectrode due to low diffusion caused by the high RTIL viscosity [50]. Well-defined ferrocene redox voltammograms were obtained in $BmimBF_4$ at conventional and microdisc platinum and glassy carbon electrodes and a concentration-dependent diffusion coefficient of ferrocene was observed [52,28]. Solvent contamination with inorganic ions misshaped the ferrocene redox peaks at the Pt microdisc electrode [28].

The results obtained suggest that the electrochemical redox mechanism is different in the various ionic liquids studied. Nevertheless, benzoyl and acetyl ferrocenes can be characterised electrochemically in these RTILs, although a fast electrode process can barely be observed due to the diffusion limitations of the high viscosity of the RTILs, as observed in most ionic liquids [27].

3.2.2. Electrochemical behaviour of CuHCF modified carbon film electrodes in RTILs

Copper hexacyanoferrate was deposited onto carbon film electrodes from aqueous solution containing $CuCl_2$, $K_3Fe(CN)_6$ and KCl at pH 2.8 by chemical adsorption. After the film-modified electrode was dried and stabilised for 1 day at room temperature in air, it was characterised in $BmimNTF_2$ and $BpyrNTF_2$ (no CuHCF redox peaks were obtained in $BmimNO_3$). Note that copper hexacyanoferrate

could not be deposited from RTIL solutions since the solubility of inorganic crystalline salts is very low due to low solvation of the ions by the rather large solvent species as well as the high viscosity of the ionic liquids [53]. CuHCF is often used as a mediator in sensors [35,54] and biosensors [41] and it was characterised in RTILs in order to test the possibility of using RTILs as the electrolyte in sensing or biosensing systems.

As is seen from Fig. 8, cyclic voltammograms in aqueous solution, and in ionic liquids, were different from each other. Well-defined peaks were obtained in aqueous solution, with peak current densities up to 2 mA cm^{-2}, whilst these values were more than 100 times lower in RTILs, caused by a slow or impossible (in the case of $BmimNO_3$) charge compensation process due to the bigger size of the charge compensating cation and the higher viscosity of the liquids. The peak separation was also much bigger in RTIL solutions for the same reason. The oxidation peak of Fe^{II} was at ~+1.2 V and the position of the reduction peak of Fe^{III} depended on the liquid: 0.5 V in $BmimNTF_2$ or 0.75 V in $BpyrNTF_2$. Moreover, the redox peaks were less well-defined in ionic liquids than in aqueous solution. Nevertheless, the Fe^{II}/Fe^{III} redox couple was clearly visible in the CVs at CuHCF modified electrodes in both RTILs so that they do show some potential for use as electrolytes in sensing systems with CuHCF as redox mediator.

3.2.3. Polymerisation of neutral red

Neutral red is a phenazine dye which is soluble in water and ethanol. Recently, electropolymerised neutral red, or poly(neutral red) (PNR), has been used as a redox mediator in some sensors [55–57] and biosensors [58–61]. The use of RTILs for sensors and biosensors is an important type of application that would decrease the number of reagents usually used, since no electrolyte is required. One of the possibilities would be preparation of the mediator, such as PNR, directly in ionic liquids.

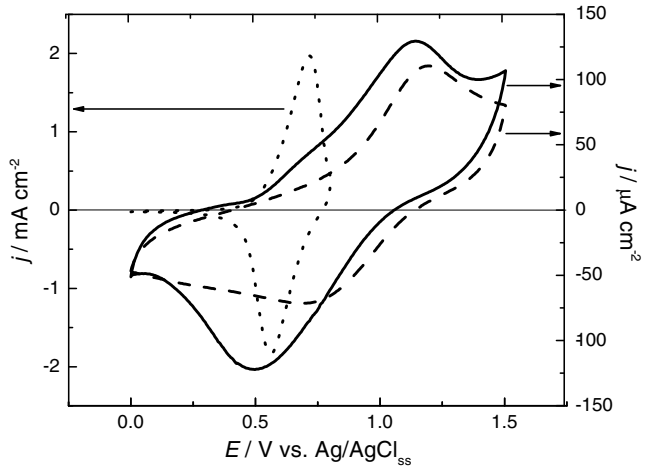

Fig. 8. Cyclic voltammograms at carbon film electrode chemically modified with CuHCF. Supporting electrolytes: (·····) 0.1 M KCl aqueous solution, (——) $BmimNTF_2$, and (– – – –) $BpyrNTF_2$. Scan rate 50 mV s^{-1}.

Polymerisation was performed from a solution of 3 mM neutral red monomer in the RTIL. The polymerisation was carried out as in aqueous solutions, by cycling the applied potential in a potential window adjusted to each RTIL, but, in general it was between −1.0 (−1.3 V in $BmimNTF_2$) and 0.8 V (1.0 V in $BmimNO_3$) for 20 cycles. The first three cycles of these were extended by 0.3–0.5 V (until monomer oxidation was observed) in the positive direction to produce radical species which initiate polymerisation.

The CVs of the electropolymerisation, Fig. 9, are slightly different in the three RTILs, mostly due to the different solvating properties of the media, leading to different polymer growth mechanisms. The effect of the different solvent properties was also visually evident by observing the different colours of the monomer solution in the different RTILs. The solution in $BmimNTF_2$ became strong orange, in $BpyrNTF_2$ an intense rose colour, and in $BmimNO_3$ it was light brown (from initial yellow-brownish). In aqueous solutions [44], the slightly acidic NR solutions have a purple colour which does not change during polymerisation. PNR made in $BmimNO_3$ (Fig. 9a3) was the most similar to that from aqueous solutions (performed from 1 mM neutral red in 0.05 M phosphate buffer, pH 5.5, and 0.1 M KNO_3), probably due to NO_3^- that catalysed polymerisation and stabilised PNR films since it is one of the best doping anions for this polymer, as is known for aqueous solutions [52]. Unlike in aqueous solution, the reduction peak at −0.7 V decreased with the number of cycles but the oxidation peak increased significantly in height in $BmimNTF_2$ (Fig. 9a1) and $BpyrNTF_2$ (Fig. 9a2), but not in $BmimNO_3$ (Fig. 9a3). This could be due to doping of the polymer formed since NTF_2^- is a larger anion than NO_3^-.

The PNR-modified electrodes were characterised electrochemically by cyclic voltammetry in 0.1 M phosphate buffer saline (PBS), pH 7.0, aqueous solution (Figs. 9b) and in the same RTILs (see insets) between −1.0 and 1.0 V. Although the polymerisation seemed to be better in $BmimNO_3$, the CV in aqueous solution most similar to that of PNR formed in aqueous solution [44] was obtained for PNR made in $BmimNTF_2$ – nevertheless, the peak current was ~50 µA cm^{-2} lower and peaks, as for PNR obtained in all RTILs, were shifted towards more positive potentials. No neutral red oxidation peaks were obtained at PNR films deposited from either $BpyrNTF_2$ or $BmimNO_3$, but they exhibited a much higher oxidation current at more positive potentials (0.8–0.9 V) where irreversible neutral red oxidation can occur.

CVs of PNR-modified electrodes in the same RTILs in which they were prepared had much lower peak currents than in aqueous solution, related to higher viscosity and lower RTIL conductivity [27] and ingress/egress of counter ions. Moreover, only PNR in $BmimNTF_2$ gave a similar CV to that obtained in aqueous solution. The other two RTILs exhibited no clear neutral red reduction peak and,

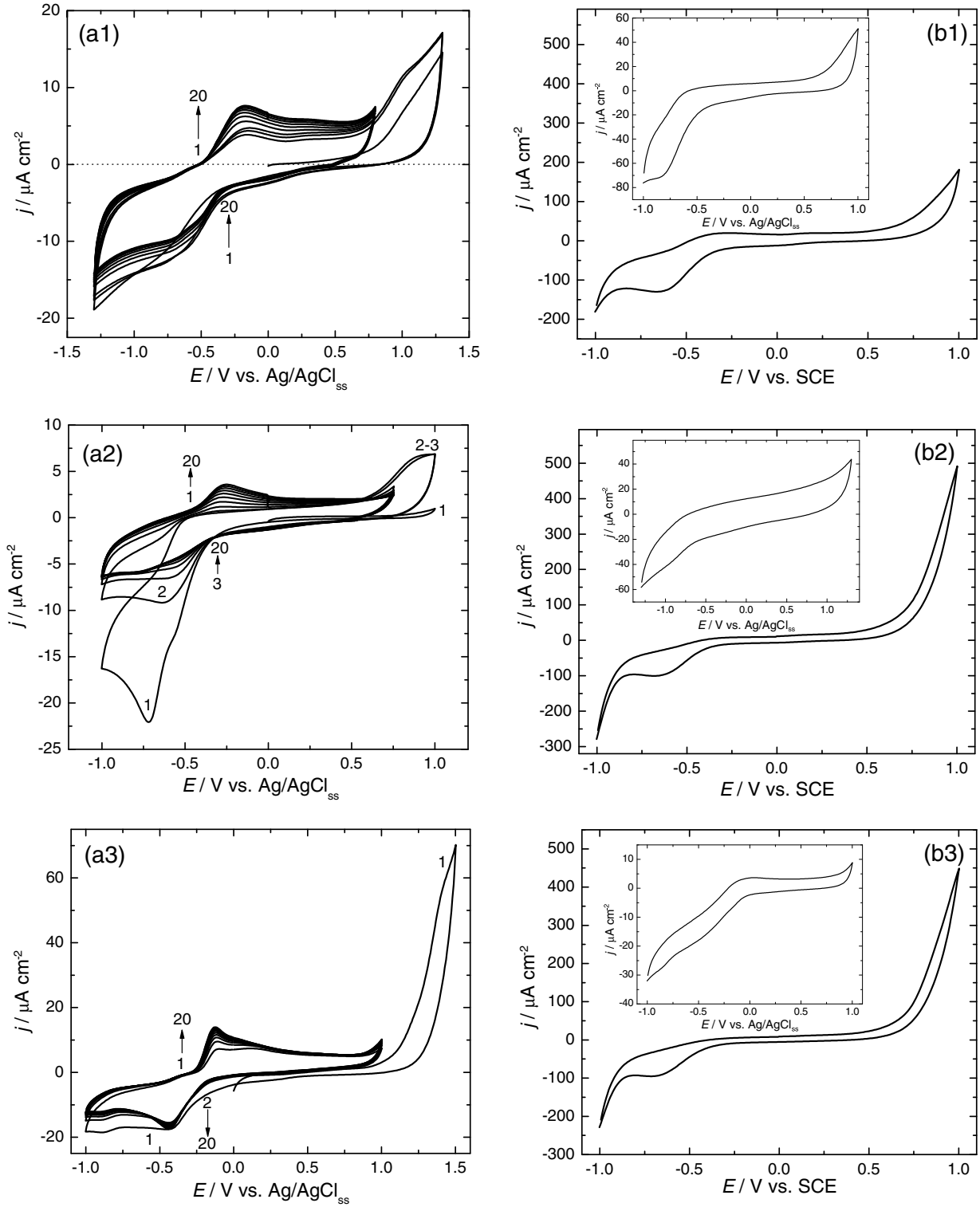

Fig. 9. (a) CVs of neutral red polymerisation from 3 mM of the monomer in (a1) $BmimNTF_2$, (a2) $BpyrNTF_2$ and (a3) $BmimNO_3$. (b) CVs of PNR in 0.1 M PBS, pH 7.0 aqueous solution; PNR prepared in (b1) $BmimNTF_2$, (b2) $BpyrNTF_2$ and (b3) $BmimNO_3$. Insets represent CVs of the same films in corresponding RTILs. Scan rate 10 mV s^{-1}.

in the case of $BmimNO_3$, the oxidation peak was at a much more positive potential.

PNR-modified carbon film electrodes deposited from aqueous solution exhibited similar voltammetric behaviour to that in aqueous solution in both $BmimNTF_2$ and $BpyrNTF_2$ (not shown) although the peak current was ~5 times lower. However, these PNR films were not stable in any of the RTILs at such high positive potentials as in aque-

ous solutions, and the current rapidly decreased with the number of cycles from −1.0 V to +1.0 V until the film was completely removed. The typical colour of the film disappeared, and CVs recorded afterwards in buffer showed a bare carbon film. These experiments showed that PNR dissolves in RTILs when a positive potential of more than +0.5 V is applied, but are not affected at less positive potentials or in the negative potential region. Since PNR-mediated biosensors operate in the negative potential region with oxidases [58,59,61] they can, in principle, be used in the RTIL medium for biosensing applications, as has been shown [62]. Further work will therefore investigate applying RTILs to electrochemical PNR-mediated biosensors.

4. Conclusions

The electrochemical behaviour of carbon film electrodes in three room temperature ionic liquids, $BmimNTF_2$, $BpyrNTF_2$, and $BmimNO_3$, was studied by cyclic voltammetry and electrochemical impedance spectroscopy. Oxygen reduction interferes in the electrochemical processes; after oxygen removal, the potential window at carbon film electrode was between −2.0 V and 2.0 V in $BmimNTF_2$, −2.5 V and 2.0 V in $BpyrNTF_2$, and −1.7 V and 1.5 V vs. $Ag/AgCl_{ss}$ in $BmimNO_3$.

The RTILs were applied to the electrochemical investigation of some potential redox mediators: ferrocene derivatives, exemplified by benzoyl- and acetyl-ferrocene, that are insoluble in water and cannot be investigated in aqueous solutions, CuHCF and PNR. For the ferrocenes, quasi-reversible behaviour in $BpyrNTF_2$ and $BmimNO_3$, and irreversibility in $BmimNTF_2$, was found. Regarding CuHCF, poor reversibility, and much lower currents, were found compared to aqueous solution due to diffusion limitations caused by the higher viscosity and the lower conductivity of RTILs.

Polymerisation of neutral red in the RTILs occurred in a slightly different way to that in aqueous solutions; the most similar polymerisation was in $BmimNO_3$. It was also observed that PNR dissolved when potentials more positive than +0.5 V were applied. However, application as a mediator for sensors and biosensors is usually at negative or less positive values of applied potential, so that further investigation of biosensor performance in RTILs will be carried out.

Acknowledgements

Financial support from Fundação para a Ciência e Tecnologia (FCT), ICEMS (Research Unit 103) are gratefully acknowledged. Prof. H. D. Liess is thanked for the gift of the electrical resistors.

References

[1] T. Welton, Coord. Chem. Rev. 248 (2004) 2459.
[2] S. Park, R.J. Kazlauskas, Curr. Opin. Biotechnol. 14 (2003) 432.
[3] M.C. Buzzeo, R.G. Evans, R.G. Compton, Chem. Phys. Chem. 5 (2004) 1106.
[4] J. Zhang, A.M. Bond, Analyst 130 (2005) 1132.
[5] C.A. Brooks, A.P. Doherty, Electrochem. Commun. 6 (2004) 867.
[6] A.P. Doherty, C.A. Brooks, Electrochim. Acta 49 (2004) 3821.
[7] U. Schröder, J.D. Wadhawan, R.G. Compton, F. Marken, P.A.Z. Suarez, C.S. Consorti, R.F. de Souza, J. Dupont, New J. Chem. 24 (2000) 1009.
[8] J.D. Wadhawan, U. Schröder, A. Neudeck, S.J. Wilkins, R.G. Compton, F. Marken, C.S. Consorti, R.F. de Souza, J. Dupont, J. Electroanal. Chem. 493 (2000) 85.
[9] V.M. Hultgren, A.W.A. Mariotti, A.M. Bond, A.G. Wedd, Anal. Chem. 74 (2002) 3151.
[10] J. Zhang, A.M. Bond, W.J. Belcher, K.J. Wallace, J.W. Steed, J. Phys. Chem. B 107 (2003) 5777.
[11] E. Rozniecka, G. Shul, J. Sirieix-Plenet, L. Gaillon, M. Opallo, Electrochem. Commun. 7 (2005) 299.
[12] B. Orel, A.Š. Vuk, V. Jovanovski, R. Ješe, L.S. Perše, S.B. Hočevar, E.A. Hutton, B. Ogorevc, A. Jesih, Electrochem. Commun. 7 (2005) 692.
[13] A.I. Bhatt, A. Mechler, L.L. Martin, A.M. Bond, J. Mater. Chem. 17 (2007) 2241.
[14] J.F. Liu, J.A. Jonsson, J.B. Jiang, Trends Anal. Chem. 24 (2005) 20.
[15] M.C. Buzzeo, C. Hardacre, R.G. Compton, Anal. Chem. 76 (2004) 4583.
[16] D. Giovanelli, M.C. Buzzeo, N.S. Lawrence, C. Hardacre, K.R. Seddon, R.G. Compton, Talanta 62 (2004) 904.
[17] Y.G. Lee, T.C. Chou, Biosens. Bioelectron. 20 (2004) 33.
[18] R. Wang, T. Okajima, F. Kitamura, T. Ohsaka, Electroanalysis 16 (2004) 66.
[19] Q. Zhao, D. Zhan, H. Ma, M. Zhang, Y. Zhao, P. Jing, Z. Zhu, X. Wan, Y. Shao, Q. Zhuang, Front. Biosci. 10 (2005) 326.
[20] J.A. Laszlo, D.L. Compton, J. Mol. Catal. B 18 (2002) 109.
[21] W.Y. Lou, W.M. Zong, H. Wu, Biocatal. Biotransform. 22 (2004) 171.
[22] Y. Zhao, Y. Gao, D. Zhan, H. Liu, Q. Zhao, Y. Kou, Y. Shao, M. Li, Q. Zhuang, Z. Zhu, Talanta 66 (2005) 51.
[23] Y.Y. Liu, W.Y. Lou, W.M. Zong, R. Xu, X. Hong, H. Wu, Biocatal. Biotransform. 23 (2005) 89.
[24] M.F. Machado, J.M. Saraiva, Biotechnol. Lett. 27 (2005) 1233.
[25] X. Lu, J. Hu, X. Yao, Z. Wang, J. Li, Biomacromolecule 7 (2006) 975.
[26] Y. Liu, L. Shi, M. Wang, Z. Li, H. Liu, J. Li, Green Chem. 7 (2005) 655.
[27] M. Galiński, A. Lewandowski, I. Stępniak, Electrochim. Acta 51 (2006) 5567.
[28] S. Eisele, M. Schwarz, B. Speiser, C. Tittel, Electrochim. Acta 51 (2006) 5304.
[29] M.C. Buzzeo, C. Hardacre, R.G. Compton, ChemPhysChem 7 (2006) 176.
[30] C.M.A. Brett, L. Angnes, H.D. Liess, Electroanalysis 13 (2001) 765.
[31] O.M.S. Filipe, C.M.A. Brett, Electroanalysis 16 (2004) 994.
[32] O.M.S. Filipe, C.M.A. Brett, Talanta 61 (2003) 643.
[33] C. Gouveia-Caridade, C.M.A. Brett, Electroanalysis 17 (2005) 549.
[34] R. Pauliukaite, C.M.A. Brett, Electroanalysis 17 (2005) 1354.
[35] R. Pauliukaite, M.E. Ghica, C.M.A. Brett, Anal. Bioanal. Chem. 381 (2005) 972.
[36] C. Gouveia-Caridade, R. Pauliukaite, C.M.A. Brett, Electroanalysis 18 (2006) 854.
[37] M. Florescu, C.M.A. Brett, Anal. Lett. 37 (2004) 871.
[38] M. Florescu, C.M.A. Brett, Talanta 65 (2005) 306.
[39] M.E. Ghica, C.M.A. Brett, Anal. Chim. Acta 532 (2005) 145.
[40] M.E. Ghica, C.M.A. Brett, Anal. Lett. 38 (2005) 907.
[41] R. Pauliukaite, C.M.A. Brett, Electrochim. Acta 50 (2005) 4973.
[42] M.E. Ghica, C.M.A. Brett, Electroanalysis 18 (2006) 748–756.
[43] J.J. Golding, D.R. MacFarlane, L. Spiccia, M. Forsyth, B.W. Skelton, A.H. White, Chem. Commun. (1998) 1953.

[44] R. Pauliukaite, M.E. Ghica, M. Barsan, C.M.A. Brett, J. Solid State Electrochem. 11 (2007) 899.
[45] M.C. Buzzeo, O.V. Klymenko, J.D. Wathawan, C. Hardacre, K.R. Seddon, R.G. Compton, J. Phys. Chem. A 107 (2003) 8872.
[46] C. Chiappe, D. Pieraccini, J. Phys. Chem. A 110 (2006) 4937.
[47] D.R. MacFerlane, J. Sun, J. Golding, P. Meakin, M. Forsyth, Electrochim. Acta 45 (2000) 1271.
[48] A. Lewandowski, I. Stepniak, Phys. Chem. Chem. Phys. 5 (2003) 4215.
[49] L. Kavan, L. Dunsch, ChemPhysChem 4 (2003) 944.
[50] J. Zhang, A.M. Bond, Anal. Chem. 75 (2003) 2694.
[51] R. Carvalho, A.I. Ribeiro, R. Pauliukaite, C.M.A. Brett, Unpublished data.
[52] L. Nagy, G. Gyetvai, L. Kollár, G. Nagy, J. Biochem. Biophys. Methods 30 (2006) 121.
[53] P.K. Mandal, S. Saha, R. Karmkar, A. Samanta, Curr. Sci. 90 (2006) 301.
[54] R. Pauliukaite, M. Florescu, C.M.A. Brett, J. Solid State Electrochem. 9 (2005) 354.
[55] A.A. Karyakin, E.E. Karyakina, H.L. Schmidt, Electroanalysis 11 (1999) 149.
[56] G. Broncová, T.V. Shishkanova, P. Matějka, R. Volf, V. Král, Anal. Chim. Acta 511 (2004) 197.
[57] W. Sun, K. Jiao, J. Han, L. Lu, Anal. Lett. 38 (2005) 1137.
[58] M.E. Ghica, C.M.A. Brett, Electroanalysis 18 (2006) 748.
[59] M.E. Ghica, C.M.A. Brett, Anal. Lett. 39 (2006) 1527.
[60] F. Qu, M. Yang, J. Chen, G. Shen, R. Yu, Anal. Lett. 39 (2006) 1785.
[61] R. Pauliukaite, A.M. Chiorcea Paquim, A.M. Oliveira Brett, C.M.A. Brett, Electrochim. Acta 52 (2006) 1.
[62] R. Pauliukaite, A.P. Doherty, K.D. Murnaghan, C.M.A. Brett, Electroanalysis (in press), doi:10.1002/elan.200704081.